Unraveling the Concerted Reaction Mechanism of the Noncatalyzed Mukaiyama Reaction between C,O,O-Tris(trimethylsilyl)ketene Acetal and Aldehydes Using Density Functional Theory

Hadj Mohamed, Slim; Trabelsi, Mahmoud; Champagne, Benoît

Published in:
The Journal of physical chemistry. A, Molecules, spectroscopy, kinetics, environment, & general theory

DOI:
10.1021/acs.jpca.6b02588

Publication date:
2016

THE JOURNAL OF PHYSICAL CHEMISTRY A

Article

pubs.acs.org/JPCA

Unraveling the Concerted Reaction Mechanism of the Noncatalyzed Mukaiyama Reaction between *C,O,O*-Tris(trimethylsilyl)ketene Acetal and Aldehydes Using Density Functional Theory

Slim Hadj Mohamed,[†,‡] Mahmoud Trabelsi,[†] and Benoît Champagne*[,‡]

[†]Laboratory of Natural Substances, Faculty of Sciences, University of Sfax, 3038 Sfax, Tunisia

[‡]Laboratory of Theoretical Chemistry, Theoretical and Structural Physical Chemistry Unit, University of Namur, rue de Bruxelles, 61, B-5000 Namur, Belgium

Supporting Information

ABSTRACT: The uncatalyzed Mukaiyama aldol reaction between *C,O,O*-tris(trimethylsilyl)ketene acetal and aldehydes bearing alkyl, vinyl, and aromatic substituents has been studied theoretically using density functional theory with the M06-2X exchange−correlation functional. These DFT calculations mostly demonstrate that (i) the *syn* product is both kinetically and thermodynamically favored, (ii) the diastereoselectivity of the uncatalyzed reaction is larger than observed for the reaction catalyzed by HgI_2 and it is inverted with respect to the latter, (iii) solvents with larger dielectric constants increase the activation barrier but reduce the diastereoselectivity, (iv) the concerted reaction is preferred over the stepwise reaction, and (v) the $OSiMe_3$ group in geminal lowers the activation barrier and increases the energy of reaction. Analyzing the concerted mechanism unravels four types of cyclic transition states, two pro-*anti* and two pro-*syn*. Then, the relative energy of the most stable transition state of each type as well as of the corresponding *anti* and *syn* products shows that the *syn* reaction path is located at lower Gibbs enthalpy than the *anti* reaction path for all substituents.

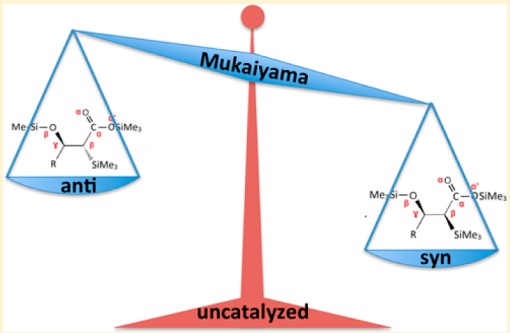

I. INTRODUCTION

The Mukaiyama aldol[1] reaction is an efficient reaction for forming carbon−carbon bonds. This reaction is an addition of silyl enol ether (enolsilane) or ketene silyl acetal on carbonyl compounds. It provides a route for the stereoselective construction of β-hydroxy carbonyl units, which are important building blocks for the preparation of a broad range of natural products and pharmaceuticals. This aldol reaction is usually catalyzed by Lewis acids but it can also proceed without catalyst when the acidity of the Si atom of the silyl enol is increased.[2−5] For instance, Bellassoued et al.[6] have carried out a noncatalyzed addition between a bis(trimethylsilyl)ketene acetal and an aromatic aldehyde under high pressure.

Mukaiyama aldol reaction has also been described using quantum chemical calculations.[4,7,8] Wong and Wong[8] have shown that the noncatalyzed condensation of the trihydrosilyl enol ether (CH_2═CH—O—SiH_3) on formaldehyde is possible via two mechanisms, concerted or stepwise and that the concerted mechanism is favored. During the concerted mechanism [ΔE = −22.7 kcal mol^{-1} and $\Delta E^{\ddagger}$ = 18.4 kcal mol^{-1}, as estimated at the G3(MP2) level of approximation] the migration of the silyl group from the enol ether to the aldehyde is accompanied by the formation of a CC single bond. The role of the silyl group is not limited to influencing the nature of the transition state because the silicon transfer from the enolsilane to the β-alkoxy position may be a key step in the overall mechanism and becomes crucial to the turnover necessary for nonstoichiometric transformations. On the contrary, in the case of the concerted mechanism, the activation energy of the first step is much larger ($\Delta E^{\ddagger}$ = 49.5 kcal mol^{-1}). These results were in agreement with previous works.[4,7,9,10] So, for the concerted mechanism of the same reaction, Gung et al.[7] obtained at the MP2/6-31G* ΔH = −33.2 kcal mol^{-1} and $\Delta E^{\ddagger}$ = 13.8 kcal mol^{-1} and highlighted that the Si atom of the transition state presents a trigonal bipyramid geometry.

Though Mukaiyama reaction between a tris-silyl ketene acetal and an aldehyde is less common than the reactions involving bis-silyl and monosilyl species, it was investigated by Bellassoued and co-workers,[6,11,12] in the case of the condensation of tris(trimethylsilyl)ketene acetal with a variety of aldehydes in the presence of Lewis acids or bases. In particular, in ref 12 they have reported on the reaction between *C,O,O*-tris(trimethylsilyl)ketene acetal **1** and a variety of aldehydes **2a−2h** (aliphatic, vinylic, and aromatic), catalyzed by HgI_2 at room temperature and in toluene solutions. This aldol reaction produces *syn* and *anti* β-(trimethylsiloxy)-α-(trimethylsilyl)alkanoic acid silyl esters **3** in low diastereose-

Received: March 12, 2016
Revised: June 18, 2016
Published: June 20, 2016

DOI: 10.1021/acs.jpca.6b02588
J. Phys. Chem. A 2016, 120, 5649−5657

Scheme 1. Mukaiyama Reaction between the *C,O,O*-Tris(trimethylsilyl)ketene Acetal 1 and Aldehydes 2a−2h (Called Reaction 1)

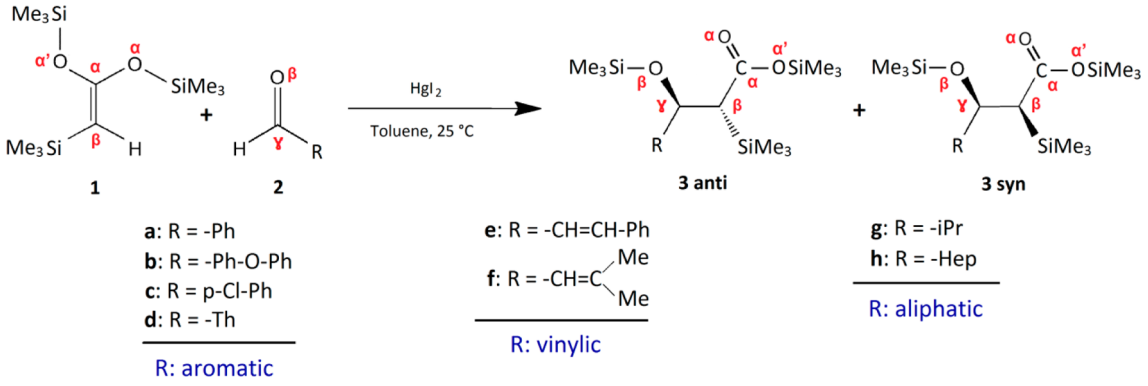

Table 1. Enthalpy ($\Delta H^{\ominus}$, kcal mol^{-1}), Entropy ($\Delta S^{\ominus}$, cal K^{-1} mol^{-1}), and Gibbs Enthalpy ($\Delta G^{\ominus}$, kcal mol^{-1}) of Reaction for the Most Stable Conformers of the 3 *anti* and 3 *syn* Diastereomers, As Determined at the M06-2X/6-31G* Level (T = 298.15K; P = 1 bar) as Well as Representative Geometrical Parameters of the Products, the $\alpha_{Si-C\beta-C\gamma-O\beta}$ and $\beta_{Si-C\beta-C\alpha-O\alpha}$ Dihedral Angles (deg) and the $d(O_{\beta}\cdots Si)$ Distances (Å)

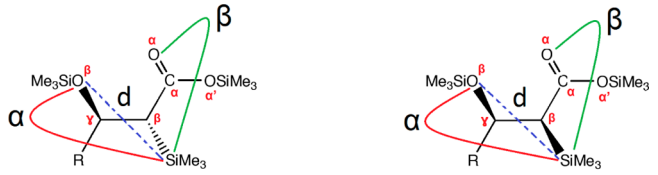

reaction	$\Delta H^{\ominus}$	$\Delta S^{\ominus}$	$\Delta G^{\ominus}$	$\alpha_{Si-C\beta-C\gamma-O\beta}$	$\beta_{Si-C\beta-C\alpha-O\alpha}$	$d(O_{\beta}\cdots Si)$
1 + **2a** → **3a** *anti*	−36.79	−52.82	−21.04	178.3	83.0	4.153
1 + **2a** → **3a** *syn*	−37.36	−52.42	−21.73	52.0	79.9	3.018
1 + **2b** → **3b** *anti*	−36.03	−50.95	−20.84	179.7	83.0	4.150
1 + **2b** → **3b** *syn*	−37.53	−52.69	−21.82	50.7	80.2	3.002
1 + **2c** → **3c** *anti*	−37.19	−51.11	−21.95	178.5	83.8	4.154
1 + **2c** → **3c** *syn*	−38.13	−52.62	−22.44	52.1	84.7	3.013
1 + **2d** → **3d** *anti*	−37.31	−52.76	−21.58	178.7	82.9	4.149
1 + **2d** → **3d** *syn*	−37.54	−52.69	−21.83	51.9	84.2	3.016
1 + **2e** → **3e** *anti*	−34.74	−50.38	−19.72	180.8	85.9	4.150
1 + **2e** → **3e** *syn*	−35.42	−55.11	−18.99	−42.3	111.6	3.034
1 + **2f** → **3f** *anti*	−34.04	−52.05	−18.52	180.9	81.1	4.146
1 + **2f** → **3f** *syn*	−34.82	−53.73	−18.80	−43.8	114.3	3.045
1 + **2g** → **3g** *anti*	−39.10	−60.64	−21.02	181.7	88.5	4.164
1 + **2g** → **3g** *syn*	−40.10	−56.21	−23.34	43.3	78.5	2.920
1 + **2h** → **3h** *anti*	−39.24	−60.71	−21.14	182.7	89.6	4.164
1 + **2h** → **3h** *syn*	−40.38	−64.30	−21.21	−39.8	110.3	3.037

lectivity, of which the major diastereoisomer is **3** *anti* and the minor is **3** *syn* (Scheme 1).

In this work, density functional theory (DFT) is employed to describe this Mukaiyama condensation but in the absence of catalyst. By determining the structural, electronic, and thermodynamical properties of the reactants, transition states, and products as well as by using reactivity criteria, we address several issues, including (i) which $SiMe_3$ group is migrating, (ii) which product, *syn* or *anti*, is favored, (iii) how the presence of one, two, and three silyl groups impacts the reactions, and (iv) what are the differences with respect to the experimental HgI_2 catalyzed reaction,[12] and with respect to other investigations.[4,7,8] The work is organized as follows: the details on the computational procedure are described in the next section; the results are then presented and discussed for the reactants, the energies of reaction, and the concerted mechanism; finally, we conclude.

II. COMPUTATIONAL METHODS

Equilibrium structures of reactants and products were optimized at the DFT level using the M06-2X exchange−correlation functional[13,14] and the 6-31G(d) basis set. For the products, the (2*R*,3*R*) absolute configuration is chosen to represent the *anti* form whereas the *syn* form is represented by the (2*R*,3*S*) configuration. For both products forms, several starting structures were considered in the geometry optimization to probe widely the potential energy surface and to locate the different minima. These structures were obtained by considering systematic rotations, by steps of 30°, around the $C_{\beta}-C_{\gamma}$ bond. The transition states (TS) were localized and

DOI: 10.1021/acs.jpca.6b02588
J. Phys. Chem. A 2016, 120, 5649−5657

characterized using the same M06-2X/6-31G* level of approximation. They possess a unique imaginary frequency. Intrinsic reaction coordinate (IRC) calculations were then performed to check that the TS are related to the corresponding reactants and products. For all species, reactants, products, and TS, the standard enthalpy ($\Delta H^{\ominus}$, $\Delta H^{\ddagger}$), entropy ($\Delta S^{\ominus}$, $\Delta S^{\ddagger}$), and Gibbs enthalpy ($\Delta G^{\ominus}$, $\Delta G^{\ddagger}$) were evaluated (T = 298.15 K, P = 1 atm).

Several descriptors[15−22] of the electronic structure and reactivity were evaluated, including the energies of the highest occupied molecular orbital (HOMO, ε_H) and of the lowest unoccupied molecular orbital (LUMO, ε_L), the LUMO−HOMO gap (gap = $\varepsilon_{LUMO} - \varepsilon_{HOMO}$), the electronegativity [$\chi = -(\varepsilon_{HOMO} + \varepsilon_{LUMO})/2$], the chemical potential ($\mu = -\chi$), the global hardness [$\eta = (\varepsilon_{LUMO} - \varepsilon_{HOMO})/2$], the global softness ($S = 1/2\eta$), the global electrophilicity ($\omega = \mu^2/2\eta$), the nucleophilicity index [$N(X) = \varepsilon_{HOMO}(X) - \varepsilon_{HOMO}(TCE)$, where tetracyanoethylene (TCE) is taken as reference], the local electrophilicity of atom k [$\omega_k = \omega f_k^+$, where $f_k^+ = \{q(k,N+1) - q(k,N)\}$], and the local nucleophilicity [$N_k = Nf_k^-$, where $f_k^- = \{q(k,N) - q(k,N-1)\}$]. $q(k,N)$ is the Mulliken charge on atom k of the neutral molecule containing N electrons whereas the corresponding charges for the cation and anion are $q(k,N-1)$ and $q(k,N+1)$, respectively. The ionization energy of **1** as well as the electroaffinitives of **2a−2h** were also calculated from difference energy calculations, after evaluating the energies of the cation and anion at the geometries of the neutral molecule.

Solvent effects (toluene) were taken into account both in the geometry optimizations and in the calculations of the thermodynamic state functions by using the integral equation formalism (IEF) version of the polarizable continuum model (IEF-PCM).[23] Additional calculations were carried out with acetone as solvent and *in vacuo*. All calculations were performed using the Gaussian 09 package.[24]

III. RESULTS AND DISCUSSION

Reactants Properties. After the geometrical structures were optimized, the descriptors of the reactants were calculated (Table S1), which gives a first estimate of their reactivity. The hardness (and softness) of **1** and **2a−2h** are similar, which is in favor of their interactions. The chemical potential of **1** (−2.65 eV) is larger than those of **2a−2h** (from −3.95 to −4.69 eV), confirming the transfer of electron from the *C,O,O*-tris-(trimethylsilyl)ketene acetal **1** to the aldehydes **2a−2h**. This is consistent with (i) the higher HOMO energy of **1** (−7.10 eV) than those of **2a−2h** (from −7.85 to −8.70 eV), with (ii) the larger electrophillicity index of **2a−2h** (from 1.56 to 3.01 eV) than **1** (0.77 eV), and with (iii) the smaller value of [$\Delta E_{SA} = \varepsilon_{HOMO}(\mathbf{1}) - \varepsilon_{LUMO}(\mathbf{2a-2h})$] with respect to [$\Delta E_{AS} = \varepsilon_{HOMO}(\mathbf{2a-2h}) - \varepsilon_{LUMO}(\mathbf{1})$]. This indicates a preference of interaction between the HOMO of the *C,O,O*-tris-(trimethylsilyl)ketene acetal and the LUMO of the aldehyde (Figure 1, Figure S1). This latter result is consistent with the work of Wong and Wong.[8]

Then, the local nucleophilicity values for C_α and C_β of **1** shows that the nucleophilic ionic addition (NIA) will take place between the C_γ of the aldehyde and C_β of the acetal, which has a nucleophilicity index 2 times larger than the C_α. The electroaffinities are negative for all the aldehydes. Still, these are smaller (in absolute value) for the alkyl substituents [|EA| = 0.30 and 0.22 eV for **2g** (R = isopropyl) and **2h** (R = heptyl), respectively], which also display the smallest electrophilicity indices. On the contrary, the aromatic and vinylic aldehydes have similar and quite large EA's. The increasing order of the EA's is

$$EA(\mathbf{2h}) < EA(\mathbf{2g}) < EA(\mathbf{2f}) < EA(\mathbf{2d}) < EA(\mathbf{2b}) < EA(\mathbf{2a}) < EA(\mathbf{2c}) < EA(\mathbf{2e})$$

The smaller EA of the aldehydes with alkyl substituents than for the aromatic and vinylic ones is associated with smaller electronegativity, larger hardness, and smaller global electrophilicity but the local electrophilicity on C_γ is similar to those of the aromatic substituents and larger than these of the vinylic ones.

Energies of Reaction. The enthalpies, entropies, and Gibbs enthalpies of reactions are listed in Table 1 for the most stable conformers of the **3** *anti* and **3** *syn* diastereoisomers. All reactions are exothermic and exergonic, and they are characterized by entropy reduction, owing to the formation of an additional bond. Moreover, the formation of the *anti* diastereoisomers is slightly less exothermic than for the *syn* ones. The enthalpy of reaction is the largest (in amplitude) for the alkyl substituents, with values ∼2 kcal mol^{-1} larger than those of the aromatic substituents and ∼4 kcal mol^{-1} larger than those of the vinylic ones. On the contrary, the entropies of reactions are similar for the aromatic and vinylic substituents and smaller than those of the alkyl substituents by about 8−10 cal K^{-1} mol^{-1}. As a result, there are few variations among the Gibbs enthalpies of reactions for the alkyl and aromatic substituents, but their amplitudes are typically 2 kcal mol^{-1} larger than those of the vinylic ones. Analysis of these energies at the light of the descriptors of Table 1 shows that there is no fully consistent relationship with the molecular descriptors, though the vinylic aldehydes have smaller local electrophilicities and the aliphatic ones have the largest ΔE_{SA}.

The geometry of the most stable conformation of **3** *anti* and **3** *syn* was characterized by two dihedral angles ($\alpha_{Si-C\beta-C\gamma-O\beta}$ and $\beta_{Si-C\beta-C\alpha-O\alpha}$) as well as the distance $d(O_\beta\cdots Si)$ (Table 1). The **3** *anti* products always display larger $d(O_\beta\cdots Si)$ distances than **3** *syn*, the differences in the $\beta_{Si-C\beta-C\alpha-O\alpha}$ angle between **3** *anti* and **3** *syn* are generally small, whereas the differences in $\alpha_{Si-C\beta-C\gamma-O\beta}$ angle are very important. Note that the $\alpha_{Si-C\beta-C\gamma-O\beta}$ angle is in the antiperiplanair domain for **3** *anti* {$\alpha \in [178.3°, 182.7°]$} and in the synclinal domain for **3** *syn* {$|\alpha| \in [39.8°, 52.1°]$}.

These data on the energetics of the uncatalyzed Mukaiyama aldol reaction between **1** and **2a−2h** further substantiate the role of the substituent, as pointed out by Wong and Wong.[8] Indeed, in the latter study, considering a broad range of donor/acceptor substituents on the trihydrosilyl enol ether (CH_3, NH_2, OH, F, SH, and CHO) and on the formaldehyde (CH_3, CF_3, NH_2, F, CHO, $COOCH_3$, $CH{=}CH_2$, and C_6H_5), $\Delta H^{\ominus}$ was found to vary from −2.9 to −38.7 kcal mol^{-1} whereas the energy barrier was from 7.2 to 31.3 kcal mol^{-1}. In general, acceptor/donor groups on the aldehyde reduce/increase the barrier of activation and lead to larger/smaller exothermicity. More precisely, the $\Delta H^{\ominus}$(alkyl) < $\Delta H^{\ominus}$(aromatic) < $\Delta H^{\ominus}$(vinylic) order results from donor character of the aromatic and mostly of the vinylic groups. This order was already observed for the model reactants of ref 7, but their amplitudes are smaller as a result of the absence of an additional $OSiMe_3$ group in geminal position (*vide infra*). Moreover, Denmark et al.[4] reported that the rate of the uncatalyzed aldol reaction was highly dependent on the

DOI: 10.1021/acs.jpca.6b02588
J. Phys. Chem. A 2016, 120, 5649−5657

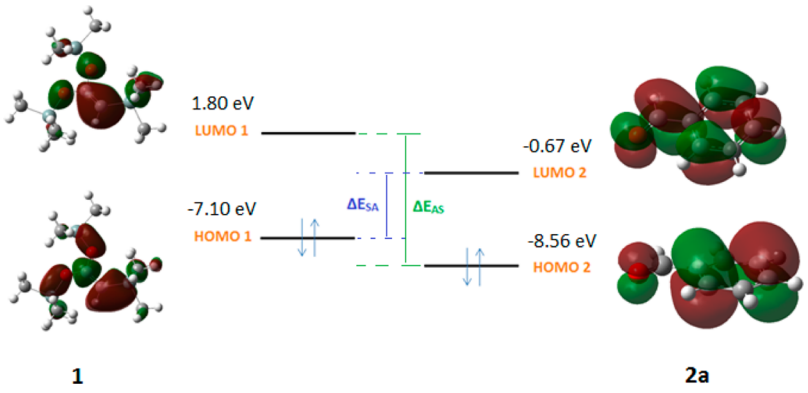

Figure 1. Relative energy positions and topologies of the frontier orbitals. The **2a** aldehyde has been chosen. $\Delta E_{SA} = \varepsilon_{HOMO}(\mathbf{1}) - \varepsilon_{LUMO}(\mathbf{2})$ and $\Delta E_{AS} = \varepsilon_{HOMO}(\mathbf{2}) - \varepsilon_{LUMO}(\mathbf{1})$.

Scheme 2. Concerted versus Stepwise Mechanisms of the Noncatalyzed Mukaiyama Reaction

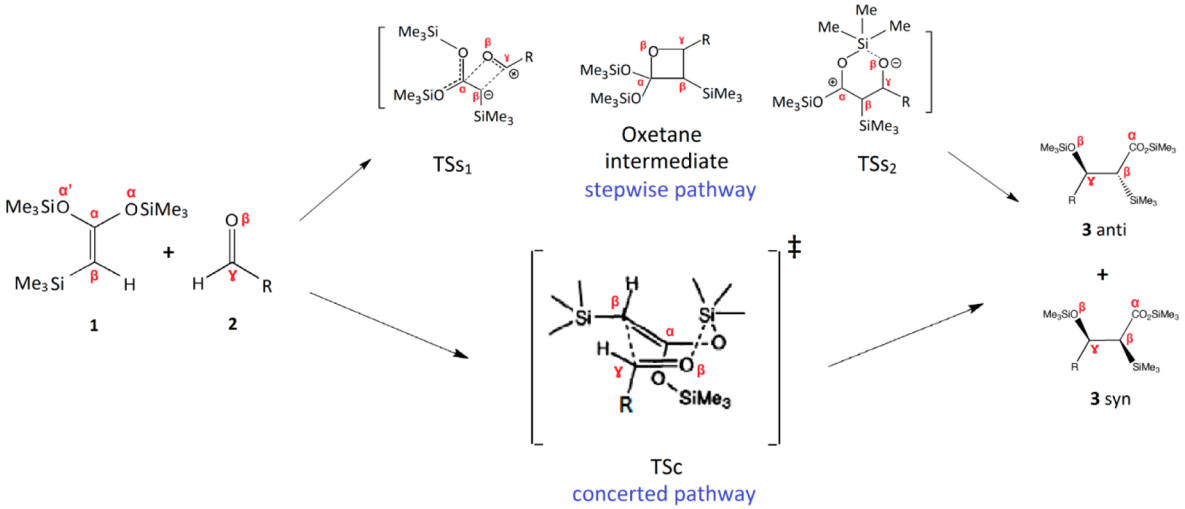

spectator substituent on the silicon atom and on the geometry of the ketene acetal.

Concerted Mechanism. The concerted mechanism of the noncatalyzed Mukaiyama reaction between the *C,O,O*-tris-(trimethylsilyl)ketene acetal **1** and aldehyde **2** involves the migration of a $SiMe_3$ group from the O_α or O_α' oxygen of the acetal to the O_β oxygen together with the formation of the C_β–C_γ bond to obtain the *syn* and *anti* diastereoisomers of *β*-(trimethylsiloxy)-*α*-(trimethylsilyl)alkanoic acid silyl esters **3** (Scheme 2). However, there are two $SiMe_3$ groups that could migrate on the oxygen of the carbonyl and one of the issues is to determine which one is transferred. Indeed, the O_α–$SiMe_3$ and O_α'–$SiMe_3$ groups have different chemical environments because the O_α'–$SiMe_3$ group is on the same side as the $SiMe_3$ group attached to C_β whereas the O_α–$SiMe_3$ one is on the opposite site. The transition state of both pro-*anti* and pro-*syn* forms, leading respectively to the *anti* and *syn* products, adopts a boat conformation (C_β–C_α–O_α–Si–O_β–C_γ).[4,7,8] There are two possible positions for the carbonyl, on the same or on the opposite side to the C_β–$SiMe_3$, as characterized by two dihedral angles, $\Theta_{Si-C\beta-C\gamma-O\beta}$ (position of the $C_\gamma O_\beta$ carbonyl with respect to $C_\beta SiMe_3$) and $\text{Ø}_{C\alpha-C\beta-C\gamma-O\beta}$ (position of the $C_\gamma O_\beta$ carbonyl with respect to the $C_\alpha C_\beta$ double bond). The Burgi–Dunitz[25] angle ($\alpha_{BD} = \alpha_{C\beta-C\gamma-O\beta}$) as well as the $d_1(O_\beta\cdots Si)$, $d_2(C_\gamma\cdots C_\beta)$, and $d_3(O_\alpha/O_{\alpha'}\cdots O_\beta)$ distances are additional descriptors of the transition states. The Ø and Θ angle values enable to distinguish between four types of transition states (T_a–T_d, Scheme 3). T_a and T_b are pro-*anti* whereas T_c and T_d are pro-*syn*. Then, T_a and T_d correspond to the situation where the carbonyl and C_β–$SiMe_3$ are on the same side whereas they are on opposite sides in T_b and T_c (Scheme 3). During the concerted mechanism, the $C_\gamma O_\beta$ carbonyl and the $C_\alpha C_\beta$ double bond are always on the same side, characterized by a $\text{Ø}_{C\alpha-C\beta-C\gamma-O\beta}$ angle ($\in[13.7°, 72.4°]$) in the synperiplanar or synclinal domain. These synperiplanar and synclinal conformations correspond to small distances between the carbonyl oxygen atom and the migrating $SiMe_3$ group whereas antiperiplanar conformations (not shown in Scheme 3) would lead to excessive distances to allow $SiMe_3$ migration. Energies, thermodynamic state functions, and key geometrical parameters of the transition states are listed in Table 2.

In the pro-*anti* case, T_a is characterized by smaller $d_1(O_\beta\cdots Si)$ and larger $d_2(C_\gamma\cdots C_\beta)$ bond lengths than T_b. For the pro-*syn* case, the situation depends on the nature of R and the differences are smaller than for the pro-*anti* case. So, if R is aromatic, T_d is characterized by larger $d_1(O_\beta\cdots Si)$ and smaller $d_2(C_\gamma\cdots C_\beta)$ bond lengths than T_c whereas if it is vinylic (or R = heptyl), the opposite is observed. Finally, when it is an isopropyl, both bond lengths are larger in the case of T_c. Further analysis of the geometrical structures of the transition states shows that both dihedral angles increase from T_a to T_b whereas from T_d to T_c, Ø decreases and Θ increases.

DOI: 10.1021/acs.jpca.6b02588
J. Phys. Chem. A 2016, 120, 5649–5657

Scheme 3. Conformation Types (a–d) of the Pro-*anti* and Pro-*syn* Transition States

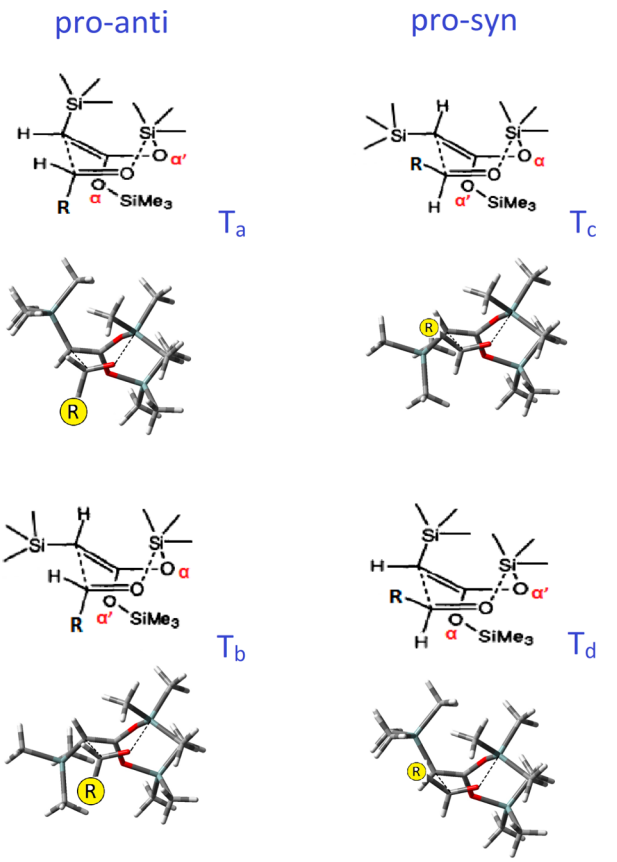

In the case of the pro-*anti* route, due to severe steric hindrance between the $SiMe_3$ attached to the C_β and the methyls of the migrating $SiMe_3$ group on the bow of the boat, the activation energies ($\Delta E^{\ddagger}$, $\Delta H^{\ddagger}$, and $\Delta G^{\ddagger}$) are systematically smaller for the T_b transition state forms than for the T_a ones, for all kinds of substituents, so that the concerted mechanism leading to the formation of the **3** *anti* diastereoisomers favors the T_b transition state (synclinal). This corresponds to the migration of the $SiMe_3$ group attached to O_α to the O_β oxygen of the carbonyl. Similarly, the T_c transition states of the pro-*syn* route are more stable than the T_d ones so that the **3** *syn* products result also from the migration of the $SiMe_3$ group attached to O_α. Nevertheless, the T_b–T_a activation energy differences are always smaller than the corresponding T_c–T_d ones.

Pro-*anti* versus Pro-*syn*. For all substituents, the following ordering of the transition state energies (E, H, and G) is observed:

$$\Delta^{\neq}(T_c,syn) < \Delta^{\neq}(T_b,anti) < \Delta^{\neq}(T_a,anti) < \Delta^{\neq}(T_d,syn)$$

so that globally, the *syn* diastereoisomers are favored over the *anti* analogs. The smaller activation energies of the pro-*syn* (T_c) transition state than the pro-*anti* (T_b) is not straightforward to explain because in T_c the $O_\beta Si$ distance is smaller (closer to the product) but the $C_\gamma C_\beta$ distance is larger. Still, it is observed that by going from T_b to T_c the Ø torsion angle decreases strongly and accordingly the $O_\alpha \cdots O_\beta$ distance, leading to an increased interaction between the frontier orbitals where the donor and acceptor are in favorable position.[26] In addition, α_{BD} decreases by about 1° from T_b to T_c. Moreover, because the energies of the **3** *anti* products are also larger than those of the *syn* species, the *syn* reaction path is below the *anti* reaction path (Figure 2). Note also that there is a nice correlation between the $\Delta E^{\ddagger}$ and $\Delta H^{\ddagger}$ amplitudes as well as between the $\Delta E^{\ddagger}$ and $\Delta G^{\ddagger}$ amplitudes. The kinetics of this reaction is in agreement with the *anti*/*syn* ratio of other uncatalyzed Mukaiyama aldol reactions, (i) between *O*,*O*-ketene acetal and aldehyde as studied by Denmark et al.,[4] of which the *syn* product was obtained with high diastereoselectivity (93/7 to 99/1) and (ii) between bis(trimethylsilyl)ketene acetals [$(OSiMe_3)_2C{=}CHR$] and benzaldehyde as studied by Bellassoued et al.,[6] of which the major diastereoisomer is *syn* and the minor is *anti* (the percentage of *syn* products ranges from 62% to 67% for R = Me, from 67% to 80% for R = Et, and from 80% to 84% for R = *i*Pr). On the contrary, there is an inversion of diastereoselectivity with respect to the reaction catalyzed by HgI_2.[12] Similar diastereoselectivity inversions have also been reported for Mukaiyama–Michael reactions due to catalysis by graphite oxide[27] and for hydroborations of acyclic allylic alcohol derivatives catalyzed by catecholborane.[28]

Stepwise versus Concerted Mechanism. The preference for the concerted mechanism over the stepwise mechanism (Scheme 2) was studied by performing additional calculations for the **2a** aldehyde. The stepwise mechanism is characterized by two transition states (TSs_1 and TSs_2). The first one corresponds to a concerted but asynchronous (the C–O bond forms later than the C–C bond) formal [2 + 2] cycloaddition leading to the formation of an oxetane intermediate. The second leads to the C_α–O_β cleavage and the migration of the $SiMe_3$ group from the acetal to the oxygen of aldehyde. As shown in Figure 3, TSs_1 lies at higher energy ($\Delta E^{\ddagger}$ = 15.8 kcal mol^{-1}, $\Delta H^{\ddagger}$ = 17.6 kcal mol^{-1}, $\Delta G^{\ddagger}$ = 35.2 kcal mol^{-1}) than the transition state of the concerted mechanism (TSc, $\Delta E^{\ddagger}$ = 11.4 kcal mol^{-1}, $\Delta H^{\ddagger}$ = 12.9 kcal mol^{-1}, $\Delta G^{\ddagger}$ = 31.0 kcal mol^{-1}). These results are in qualitative agreement with the study of Wong and Wong[8] on the uncatalyzed reaction between formaldehyde and trihydrosilyl enol ether.

Effects of the $SiMe_3$ Groups. Additional reaction profiles were then characterized to highlight the role of the $SiMe_3$ groups (Scheme 4). In reaction 2 the $SiMe_3$ substituent attached to C_β is missing whereas in reaction 3 one of the $OSiMe_3$ has been removed. Finally, in reaction 4 both are removed. ΔH of activation and of reaction, listed in Table 3, highlight the minor role of the $SiMe_3$ substituent (reaction 1 versus reaction 2) but the huge impact of the geminal $OSiMe_3$ group that reduces the activation energy by a factor of 2 and enhanced the exothermicity by about 60%. Additional calculations not detailed here demonstrate that for these simplified acetals the concerted mechanism is also favored over the stepwise one with $\Delta\Delta H^{\ddagger}$ that increase up to 12 kcal mol^{-1} when the geminal $OSiMe_3$ group is absent.

Solvent Effects. Wong et al.[8] have shown that the Mukaiyama reaction is generally favorable in solvents that do not bear donating oxygen atoms, like in dichloromethane, hexane, benzene, toluene, and acetonitrile. On the contrary, the reaction is hampered or impossible in tetrahydrofuran, diethyl ether, and *N*,*N*-dimethylformamide[1,2,29−31] whereas Kitanosona and Kobayashi have shown that the silyl enolate decomposes in the presence of water, preventing also the reaction to occur.[32] In this work, the explicit solute–solvent interactions are not investigated but the dielectric constant effects are assessed by using the PCM approach, which is an implicit solvation model. In particular, the activation energies *in vacuo* for T_b and T_c

DOI: 10.1021/acs.jpca.6b02588
J. Phys. Chem. A 2016, 120, 5649–5657

Table 2. Activation Energy ($\Delta E^{\ddagger}$, kcal mol^{-1}), Activation Enthalpy ($\Delta H^{\ddagger}$, kcal mol^{-1}), Activation Free Enthalpy ($\Delta G^{\ddagger}$, kcal mol^{-1}), and Activation Entropy ($\Delta S^{\ddagger}$, cal K^{-1} mol^{-1}) As Evaluated with the IEFPCM/M06-2X/6-31G* Method (T = 298.15 K; P = 1 bar, solvent = toluene) as Well as Representative Geometrical Parameters of the Products, the $\Theta_{Si-C\beta-C\gamma-O\beta}$ and $\emptyset_{C\alpha-C\beta-C\gamma-O\beta}$ Dihedral Angles (deg), the Burgi−Dunitz Valence Angle ($\alpha_{BD} = \alpha_{C\beta-C\gamma-O\beta}$) (deg), and the $d_1(O_\beta\cdots Si)$, $d_2(C_\gamma\cdots C_\beta)$, and $d_3(O_\alpha/O_{\alpha'}\cdots O_\beta)$ Distances (Å)[a]

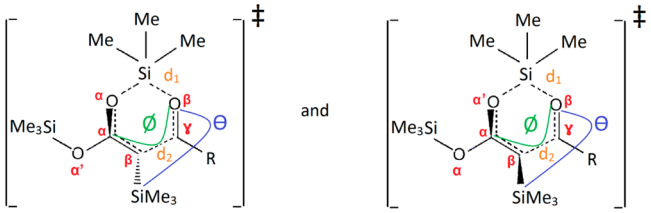

TS	$\Delta E^{\ddagger}$	$\Delta\Delta E^{\ddagger}$	$\Delta H^{\ddagger}$	$\Delta\Delta H^{\ddagger}$	$\Delta S^{\ddagger}$	$\Delta G^{\ddagger}$	$\Delta\Delta G^{\ddagger}$	Ø	Θ	α_{BD}	d_1	d_2	d_3	T
pro-**3a** *anti*-a	13.30	1.94	14.91	1.97	−60.00	32.80	2.23	17.7	251.9	107.9	2.082	2.212	2.474	a
pro-**3a** *anti*-b	11.36	0 (1.82)	12.94	0 (1.78)	−60.64	31.02	0 (1.77)	56.3	180.0	107.5	2.312	1.956	2.574	b
pro-**3a** *syn*-d	14.62	5.08	16.29	5.13	−62.85	35.03	5.78	71.5	309.3	104.8	2.149	2.142	2.600	d
pro-**3a** *syn*-c	9.54	0	11.16	0	−60.67	29.25	0	29.2	155.9	106.3	2.097	2.148	2.434	c
pro-**3b** *anti*-a	13.98	1.76	15.33	1.72	−61.31	33.61	1.47	17.6	251.9	107.7	2.065	2.211	2.469	a
pro-**3b** *anti*-b	12.22	0 (1.88)	13.61	0 (1.89)	−62.15	32.14	0 (2.21)	56.3	180.0	107.4	2.309	1.957	2.573	b
pro-**3b** *syn*-d	15.31	4.97	16.72	5.00	−64.26	35.88	5.95	71.6	309.3	104.6	2.128	2.142	2.594	d
pro-**3b** *syn*-c	10.34	0	11.72	0	−61.08	29.93	0	29.4	155.8	106.1	2.080	2.146	2.430	c
pro-**3c** *anti*-a	12.17	1.42	13.84	1.56	−62.35	32.43	1.81	17.1	250.3	108.7	2.140	2.165	2.474	a
pro-**3c** *anti*-b	10.75	0 (1.57)	12.28	0 (1.64)	−61.51	30.62	0 (1.98)	56.1	179.9	108.1	2.389	1.911	2.596	b
pro-**3c** *syn*-d	14.18	5.00	15.70	5.06	−61.75	34.11	5.47	71.0	308.7	105.4	2.187	2.128	2.614	d
pro-**3c** *syn*-c	9.18	0	10.64	0	−60.37	28.64	0	27.2	154.0	106.8	2.117	2.133	2.431	c
pro-**3d** *anti*-a	13.31	2.26	14.92	2.43	−63.36	33.81	3.06	13.7	246.9	107.8	2.107	2.180	2.466	a
pro-**3d** *anti*-b	11.05	0 (1.12)	12.49	0 (1.09)	−61.24	30.75	0 (1.65)	53.9	177.2	108.0	2.335	1.951	2.572	b
pro-**3d** *syn*-d	14.56	4.63	16.08	4.68	−61.58	34.44	5.34	70.2	307.7	105.3	2.156	2.140	2.601	d
pro-**3d** *syn*-c	9.93	0	11.40	0	−59.37	29.10	0	29.0	156.8	106.3	2.108	2.138	2.434	c
pro-**3e** *anti*-a	13.69	2.40	15.33	2.62	−62.12	33.85	3.66	19.4	252.1	108.0	2.083	2.177	2.457	a
pro-**3e** *anti*-b	11.29	0 (0.81)	12.71	0 (0.80)	−58.63	30.19	0 (1.04)	44.7	168.1	108.0	2.209	2.043	2.497	b
pro-**3e** *syn*-d	14.93	4.45	16.56	4.65	−61.75	34.97	5.82	70.9	308.8	104.3	2.087	2.140	2.573	d
pro-**3e** *syn*-c	10.48	0	11.91	0	−57.82	29.15	0	34.1	162.1	106.7	2.102	2.123	2.431	c
pro-**3f** *anti*-a	13.11	1.25	14.70	1.26	−63.52	33.64	2.38	22.5	256.9	108.6	2.033	2.185	2.445	a
pro-**3f** *anti*-b	11.86	0 (0.82)	13.44	0 (0.90)	−59.77	31.26	0 (1.86)	45.0	168.3	107.6	2.055	2.056	2.495	b
pro-**3f** *syn*-d	13.67	2.63	15.34	2.80	−63.89	34.39	4.99	72.4	309.6	104.0	2.049	2.144	2.563	d
pro-**3f** *syn*-c	11.04	0	12.54	0	−56.55	29.40	0	34.6	161.8	105.9	2.055	2.137	2.417	c
pro-**3g** *anti*-a	10.10	1.19	11.55	0.77	−62.85	30.29	1.10	20.3	243.8	108.4	2.142	2.200	2.475	a
pro-**3g** *anti*-b	8.91	0 (1.19)	10.77	0 (1.15)	−61.78	29.19	0 (0.87)	58.2	179.8	108.0	2.392	1.912	2.597	b
pro-**3g** *syn*-d	14.30	6.58	16.24	6.62	−65.34	35.72	7.40	61.3	300.9	106.9	2.094	2.116	2.529	d
pro-**3g** *syn*-c	7.72	0	9.62	0	−62.72	28.32	0	24.6	155.0	105.5	2.100	2.164	2.443	c
pro-**3h** *anti*-a	10.48	1.44	12.20	1.46	−69.56	32.94	2.73	19.4	252.1	108.7	2.134	2.191	2.476	a
pro-**3h** *anti*-b	9.04	0 (1.51)	10.74	0 (2.43)	−65.30	30.21	0 (2.07)	56.5	178.6	107.7	2.296	1.987	2.574	b
pro-**3h** *syn*-d	12.99	3.07	14.71	3.04	−64.13	33.83	3.78	70.7	308.9	103.9	2.138	2.180	2.587	d
pro-**3h** *syn*-c	7.47	0	8.31	0	−66.51	28.14	0	39.1	167.7	107.4	2.165	2.113	2.457	c

[a]Columns with $\Delta\Delta E^{\ddagger}$ ($\Delta\Delta H^{\ddagger}$ and $\Delta\Delta G^{\ddagger}$) give the differences between the two pro-*anti* and pro-*syn* cases. In parentheses are given the differences between the most stable pro-*syn* and pro-*anti* species.

Table 3. Reaction and Activation Enthalpies (kcal mol^{-1}) for the Mukaiyama Reaction between Aldehyde 2a and Simplified Acetals Derived from Compound 1 As Evaluated with the IEFPCM/M06-2X/6-31G* Method (T = 298.15 K; P = 1 bar)

	reaction 1	reaction 2	reaction 3	reaction 4
$\Delta H^{\ominus}$	−36.8	−37.5	−23.0	−23.2
$\Delta H^{\ddagger}$	12.9	10.5	23.8	22.5

transition states as well as their differences are compared to those calculated in toluene and in acetone (Table 4).

It is observed that (i) the $\Delta E^{\ddagger}$ activation energies increase with the dielectric constant of the medium for both *syn* and *anti* mechanisms by up to 2 and 3.6 kcal mol^{-1} in toluene and in acetone, respectively, (ii) in the gas phase and in solution, the T_c state remains more stable than the T_b state, keeping the *syn*/*anti* ratio larger than 1, but that (iii) the $\Delta\Delta E^{\ddagger}$ differences decrease slightly with the dielectric constant, demonstrating that the diastereoselectivity of Mukaiyama reaction is slightly reduced.

CONCLUSIONS

Theoretical investigations using density functional theory with the M06-2X functional have been performed to unravel the concerted mechanism of the uncatalyzed Mukaiyama aldol reaction between *C,O,O*-tris(trimethylsilyl)ketene acetal **1** and aldehydes **2** bearing alkyl, vinyl, or aromatic substituents. These

DOI: 10.1021/acs.jpca.6b02588
J. Phys. Chem. A 2016, 120, 5649−5657

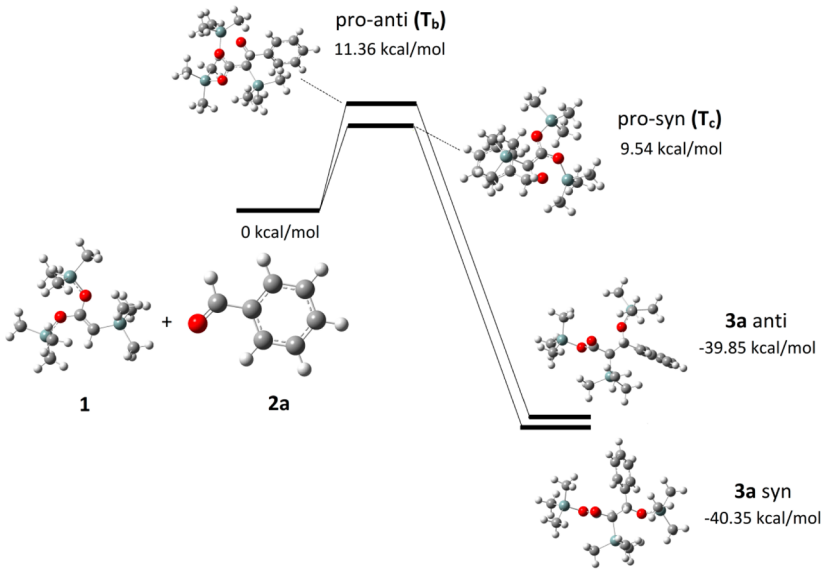

Figure 2. *anti* and *syn* reaction paths [IEFPCM(toluene)/M06-2X/6-31G(d)] for the concerted mechanism of the Mukaiyama reaction between *C,O,O*-tris(trimethylsilyl)ketene acetal **1** and aldehyde **2a**.

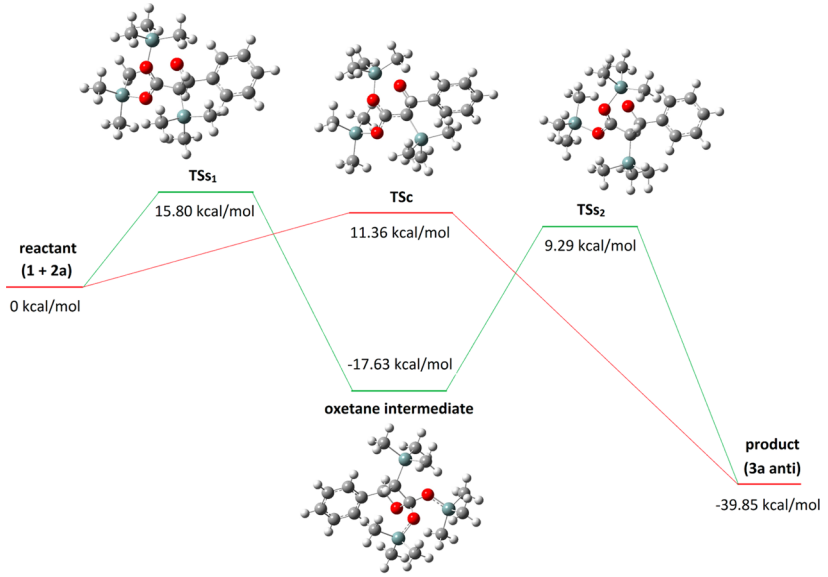

Figure 3. Energy profile [IEFPCM(toluene)/M06-2X/6-31G(d)] for the stepwise versus concerted mechanisms of the reaction between compounds **1** and **2a**.

Scheme 4. Mukaiyama Reactions between Aldehyde 2a and Acetals Derived from 1

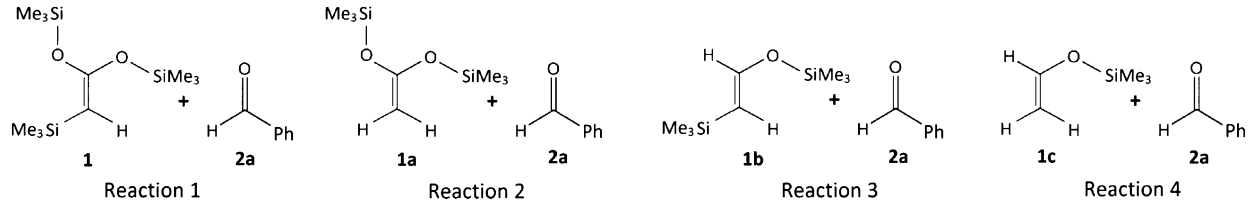

DFT calculations show that (i) the **3** *syn* product is both the kinetic and the thermodynamic product and that (ii) the diastereoselectivity of the uncatalyzed reaction is larger than observed for the reaction catalyzed by HgI_2[12] and it is inverted with respect to the latter. These calculations have substantiated the fact that solvents with larger dielectric constants increase the activation barrier but reduce the diastereoselectivity. They have also confirmed the preference for the concerted reaction over the stepwise reactions as well as the key role of the $OSiMe_3$ group in geminal on lowering the activation barrier and increasing the energy of reaction. Moreover, the study of the concerted mechanism highlights four types of cyclic transition states (T_a, T_b, T_c, T_d). The T_b conformation is the most stable pro-*anti* transition state whereas T_c is a most stable pro-*syn*.

DOI: 10.1021/acs.jpca.6b02588
J. Phys. Chem. A 2016, 120, 5649−5657

Table 4. Activation Energy ($\Delta E^{\ddagger}$, kcal mol^{-1}) for the Pro-*anti* T_b and Pro-*syn* T_c Routes As Evaluated with the IEFPCM/M06-2X/6-31G* Method (T = 298.15 K; P = 1 bar) for Different Solvation Types [*in Vacuo*, Toluene (ε_r = 2.40), and Acetone (ε_r = 21.00)] and Their Differences ($\Delta\Delta E^{\ddagger}$, kcal mol^{-1})

		in vacuo		toluene		acetone	
reaction		$\Delta E^{\ddagger}$	$\Delta\Delta E^{\ddagger}$	$\Delta E^{\ddagger}$	$\Delta\Delta E^{\ddagger}$	$\Delta E^{\ddagger}$	$\Delta\Delta E^{\ddagger}$
3a	T_b	10.16	1.88	11.36	1.82	12.05	1.19
	T_c	8.28		9.54		10.86	
3b	T_b	10.97	2.01	12.22	1.88	12.93	1.38
	T_c	8.96		10.34		11.55	
3c	T_b	9.73	1.82	10.75	1.57	11.11	0.81
	T_c	7.91		9.18		10.30	
3d	T_b	9.79	1.25	11.05	1.12	11.67	0.50
	T_c	8.54		9.93		11.17	
3e	T_b	9.76	0.82	11.29	0.81	12.61	0.75
	T_c	8.94		10.48		11.86	
3f	T_b	10.22	1.19	11.86	0.82	13.48	0.81
	T_c	9.03		11.04		12.67	
3g	T_b	7.54	1.38	8.91	1.19	9.79	0.50
	T_c	6.16		7.72		9.29	
3h	T_b	7.53	1.63	9.04	1.51	10.35	1.38
	T_c	5.90		7.47		8.97	

Both T_b and T_c correspond to the migration of the $SiMe_3$ group attached to O_α, i.e., on the opposite side to the $SiMe_3$ substituent. Then, comparison between T_b and T_c as well as between their corresponding product, **3** *anti* and **3** *syn*, leads to conclude that, for all substituents, the *syn* reaction path is located at lower energy (Gibbs enthalpy) than the *anti* reaction path.

■ ASSOCIATED CONTENT

Supporting Information

The Supporting Information is available free of charge on the ACS Publications website at DOI: 10.1021/acs.jpca.6b02588.

Chemical descriptors of the reactants; relative energy positions and topologies of the frontier orbitals for **1** + **2f** and **1** + **2g** reactants; total energies (au), imaginary frequencies (cm^{-1}), and atomic Cartesian coordinates (Å) for the reactants, transition states, and products (PDF)

■ AUTHOR INFORMATION

Corresponding Author

*B. Champagne. E-mail: benoit.champagne@unamur.be. Tel: +32 81 724554.

Notes

The authors declare no competing financial interest.

■ ACKNOWLEDGMENTS

S.H.M. thanks the Fonds Spécial de Recherche of UNamur for his Ph.D. grant. This work was supported by funds from the Belgian Government (IUAP No P7/5 "Functional Supramolecular Systems") and the Francqui Foundation. The calculations were performed on the computers of the Consortium des Équipements de Calcul Intensif, including those of the Technological Platform of High-Performance Computing, for which we gratefully acknowledge the financial support of the FNRS-FRFC (Conventions No. 2.4.617.07.F and 2.5020.11) and of the University of Namur.

■ REFERENCES

(1) Mukaiyama, T.; Narasaka, K.; Banno, K. New Aldol Type Reaction. *Chem. Lett.* **1973**, *2*, 1011−1014.

(2) Myers, A. G.; Widdowson, K. L.; Kukkola, P. J. Silicon-Directed Aldol Condensation. Evidence for a Pseudorotational Mechanism. *J. Am. Chem. Soc.* **1992**, *114*, 2765−2767.

(3) Myers, A. G.; Kephart, S. E.; Chen, H. Silicon-Directed Aldol reaction. Rate Acceleration by Small Rings. *J. Am. Chem. Soc.* **1992**, *114*, 7922−7923.

(4) Denmark, S. E.; Griedel, B. D.; Coe, D. M.; Schnute, M. E. Chemistry of Enoxysilacyclobutanes: Highly Selective Uncatalyzed Aldol Additions. *J. Am. Chem. Soc.* **1994**, *116*, 7026−7043.

(5) Miura, K.; Sato, H.; Tamaki, K.; Ito, H.; Hosomi, A. Uncatalyzed Aldol Reaction Using a Dimethylsilyl Enolate and α-Dimethylsilyl Ester in N,N-Dimethylformamide. *Tetrahedron Lett.* **1998**, *39*, 2585−2588.

(6) Bellassoued, M.; Reboul, E.; Dumas, F. High Pressure Induced Mukaiyama Type Aldol Reaction of bis Trimethylsilyl Ketene Acetals. *Tetrahedron Lett.* **1997**, *38*, 5631−5634.

(7) Gung, B. W.; Zhu, Z.; Fouch, R. A. Transition State of Silicon-Directed Aldol Reaction: An ab Initio Molecular Orbital Study. *J. Org. Chem.* **1995**, *60*, 2860−2864.

(8) Wong, C. T.; Wong, M. W. Facile Uncatalyzed Mukaiyama Aldol Reaction: An ab Initio Study of the Effects of Substituents. *J. Org. Chem.* **2005**, *70*, 124−131.

(9) Carreira, E. M. In *Comprehensive Asymmetric Catalysis*; Jacobsen, E. N., Pfaltz, A.; Yamamoto, H., Eds.; Springer Verlag: Berlin, 1999, Vol. 3, pp 996−1065.

(10) Carreira, E. M.; Fettes, A.; Marti, C. Catalytic Enantioselective Aldol Addition Reactions. *Org. React.* **2006**, *67*, 1.

(11) Bellassoued, M.; Lensen, N.; Bakasse, M.; Mouelhi, S. Two-Carbon Homologation of Aldehydes via Silyl Ketene Acetals: A New Stereoselective Approach to (E)-Alkenoic Acids. *J. Org. Chem.* **1998**, *63*, 8785−8789.

(12) Bellassoued, M.; Mouelhi, S.; Lensen, N. Two-Carbon Homologation of Aldehydes via Silyl Ketene Acetals. 2. Study of the Stereochemical Control in the Formation of (E)-Alkenoic Acid. *J. Org. Chem.* **2001**, *66*, 5054−5057.

(13) Zhao, Y.; Truhlar, D. G. Comparative DFT Study Of Van Der Waals Complexes: Rare-Gas Dimers, Alkaline-Earth Dimers, Zinc Dimer, And Zinc-Rare-Gas Dimers. *J. Phys. Chem. A* **2006**, *110*, 5121−5129.

(14) Zhao, Y.; Truhlar, D. G. The M06 Suite of Density Functionals for Main Group Thermochemistry, Thermochemical Kinetics, Noncovalent Interactions, Excited States, And Transition Elements: Two New Functional And Systematic Testing Of Four M06-Class Functionals and 12 other functionals. *Theor. Chem. Acc.* **2008**, *120*, 215−241.

(15) Parr, R. G.; Pearson, R. G. Absolute Hardness: Companion Parameter to Absolute Electronegativity. *J. Am. Chem. Soc.* **1983**, *105*, 7512−7516.

(16) Parr, R. G.; Yang, W. Density Functional Approach to the Frontier-Electron Theory of Chemical Reactivity. *J. Am. Chem. Soc.* **1984**, *106*, 4049−4050.

(17) Yang, W.; Parr, R. G.; Natl, P. Hardness, Softness, And The Fukui Function In The Electronic Theory Of Metals And Catalysis. *Proc. Natl. Acad. Sci. U. S. A.* **1985**, *82*, 6723−6726.

(18) Parr, R. G.; Yang, W. *Density Functional Theory of Atoms and Molecules*; Oxford University Press: Oxford, U.K., 1989.

(19) Parr, R. G.; Von Szentpaly, L.; Liu, S. Electrophilicity Index. *J. Am. Chem. Soc.* **1999**, *121*, 1922−1924.

(20) Chattaraj, P. K.; Maiti, B.; Sarkar, U. Philicity: A Unified Treatment of Chemical Reactivity and Selectivity. *J. Phys. Chem. A* **2003**, *107*, 4973−4975.

(21) Geerlings, P.; De Proft, F.; Langenaeker, W. Conceptual Density Functional Theory. *Chem. Rev.* **2003**, *103*, 1793−1873.

DOI: 10.1021/acs.jpca.6b02588
J. Phys. Chem. A 2016, 120, 5649−5657

(22) Domingo, L. R.; Chamorro, E.; Pérez, P. Understanding the Reactivity of Captodative Ethylenes in Polar Cycloaddition Reaction. A Theoretical Study. *J. Org. Chem.* **2008**, *73*, 4615−4624.
(23) Tomasi, J.; Mennucci, B.; Cammi, R. Quantum Mechanical Continuum Solvation Models. *Chem. Rev.* **2005**, *105*, 2999−3094.
(24) Frisch, M. J.; Trucks, G W.; Schlegel, H. B.; Scuseria, G. E.; Robb, M. A.; Cheeseman, J. R.; Scalmani, G.; Barone, V.; Mennucci, B.; Petersson, G. A.; Nakatsuji, H.; et al. *Gaussian 09*, revision A.01; Gaussian, Inc.: Wallingford, CT, 2010.
(25) Bürgi, H.-B.; Dunitz, J.; Lehn, J. M.; Wipff, G. Stereochemistry of Reaction Path at Carbonyl Centres. *Tetrahedron* **1974**, *30*, 1563−1572.
(26) Seebach, D.; Knochel, P. 2′-Nitro-2′-propen-1′-yl 2,2-Dimethylpropanoate (NPP), A Multiple Coupling Reagent. *Helv. Chim. Acta* **1984**, *67*, 261−283.
(27) Acocella, M. R.; Mauro, M.; Falivene, L.; Cavallo, L.; Guerra, G. Inverting the Diastereoselectivity of the Mukaiyama-Michael Addition with Graphite-Based Catalysts. *ACS Catal.* **2014**, *4*, 492−496.
(28) Burgess, K.; Cassidy, J.; Ohlmeyer, M. J. Substrate-Controlled Diastereoselectivities in Catalyzed and Uncatalyzed Hydroborations of Acyclic Allylic Alcohol Derivatives: Secondary Orbital Effects Involving dπ-pπ Interactions. *J. Org. Chem.* **1991**, *56*, 1020−1027.
(29) (a) Mukaiyama, T.; Banno, K.; Narasaka, K. New Cross-Aldol Reactions. Reactions of Silyl Enol Ethers with Carbonyl Compounds Activated by Titanium Tetrachloride. *J. Am. Chem. Soc.* **1974**, *96*, 7503−7509.
(30) Mukaiyama, T.; Izawa, T.; Saigo, K. Reaction of Enol Acetate with Acetal and Carbonyl Compound in the Presence of Lewis Acid. *Chem. Lett.* **1974**, 323−326.
(31) Munoz-Muniz, O.; Quintanar-Audelo, M.; Juaristi, E. Reexamination of CeCl3 and InCl3 as Activators in the Diastereoselective Mukaiyama Aldol Reaction in Aqueous Media. *J. Org. Chem.* **2003**, *68*, 1622−1625.
(32) Kitanosono, T.; Kobayashi, S. Mukaiyama Aldol Reactions in Aqueous Media. *Adv. Synth. Catal.* **2013**, *355*, 3095−3118.

DOI: 10.1021/acs.jpca.6b02588
J. Phys. Chem. A 2016, 120, 5649−5657